

Supporting information of:

Catalytic Synthesis of Boron Nitride Nanotubes at Low Temperatures

Mustafa Baysal¹, Kaan Bilge¹, Melike Mercan Yıldızhan¹, Yelda Yorulmaz¹, Çınar Öncel², Melih Papila¹, and Yuda Yürüm^{1}*

¹Sabancı University, Faculty of Engineering and Natural Sciences, Tuzla 34956, İstanbul/Turkey

² Muğla Sıtkı Kocaman University, Faculty of Engineering, Metallurgical and Materials Engineering Department B Building Kötekli Campus 48000, Muğla / TURKEY

* Corresponding author: yyurum@sabanciuniv.edu

Index:

Information about Boron oxide CVD (BOCVD) and Thermal CVD (TCVD) growth vapor trap approach

Table S1

Materials and methods

Figure S1

Figure S2

Figure S3

Figure S4

Figure S5

Figure S6

Figure S7

References

Information about Boron oxide CVD (BOCVD) and Thermal CVD (TCVD) growth vapor trap approach

The BOCVD method was designed based on a vertical induction furnace, which operates at high temperatures (1000 °C – 1700 °C) and creates a large temperature gradient. Tang et al. first introduced this method to produce BNNT by using MgO as a precursor, but catalyst role of the magnesium was not clarified¹. Later Zhi et al.² applied the method by introducing MgO and FeO precursors together as a boron oxide producer and a catalyst. Several other studies based on BOCVD were conducted aiming to produce a large quantity of BNNTs, but specific design of the experimental setup restricted its extensive usage by other research groups. In 2008 Lee et al.³ used thermal CVD method with MgO and Fe₂O₃/FeO catalyst system in a novel way by trapping precursor vapors in an inner tube which also designate the method as growth-vapor trap (GVT) TCVD. In this approach, the traditional horizontal furnace was coupled with a quartz tube to form a vacuum chamber where an inner, small quartz tube with one-end closed is placed for trapping growth vapor which allows the BNNT formation without using any sophisticated attachments (see Figure S2). Although BNNT yield was not high compared to the BOCVD, their work demonstrated that BNNTs could be grown on the substrate and inner walls of the combustion boat. Also, patterned growth of BNNTs was achieved by using catalyst coated substrates as shown in another execution of this method, with MgO designated as the most active catalyst⁴.

Table S1: Catalytic materials and temperatures used in A) BOCVD and B) TCVD methods

A

Precursors	Temperature (°C)	Catalyst	Year
¹ B, MgO	1300	Mg, Nanosized	2002
⁵ B, GaO	1550	Ga	2002
⁶ B, GaO	1550	Ga	2004
^{2, 7-9} B, MgO, and FeO	1100-1700	Fe, Mg	2005
¹⁰ B, Li ₂ CO ₃	1350	Li	2009
¹¹ B, Li ₂ O	1350	Li	2011
¹² B, MgO and SnO or FeO	1500	Mg, Fe or Sn	2014

B

Precursors	Temperature (°C)	Catalyst	Year
³ B, MgO, and FeO	1200	Mg, Nanosized	2008
⁴ B, MgO, and FeO	1100 – 1200	Mg, Fe	2010
¹³ B, NH ₄ NO ₃ , Fe ₂ O ₃	1300	Fe	2011
¹⁴ B, MgO, and FeO	1200-1400	Mg, Fe	2012
¹⁵ B, MgO, and FeO	1350	Mg, Fe	2013
¹⁶ B, Fe ₂ O ₃	900 - 1400	Fe	2013
¹⁷ B, Li ₂ O	1200	Li	2013
¹⁸ Colemanite, Fe ₂ O ₃	1280	Fe	2013
¹⁹ B, V ₂ O ₅ , Fe ₂ O ₃ and B, V ₂ O ₅ , Ni ₂ O ₃	1100	V,Fe/V,Ni	2014
²⁰ B, MgO, γ-Fe ₂ O ₃	1100 - 1200	Mg, Fe	2015
²¹ B/B ₂ O ₃ , NiY	1200	NiY	2017

Materials and Methods

Potassium ferrite (KFeO₂) synthesis

KFeO₂ was synthesized via organic precursor method. To obtain single phase KFeO₂, a specific amount of cation salts and an excess amount of organic carrier were used. Fe(NO₃)₃·9H₂O and KNO₃ were used as cation salts and citric acid (CA) as carrier material. The desired amount of each cation salt and an excess amount of CA were dissolved in distilled water separately then mixed. To homogenize the resulting mixture, the solution was stirred at 200 rpm for 30 minutes. Then, the homogenized solution was heated on the magnetic stirrer to the complete dryness. The resulting powder was collected and calcined at 700 °C for 2 hours. After two hours sample was vacuum quenched immediately in the desiccator without allowing cooled slowly in the oven. Final olive green KFeO₂ powder was collected and stored in the glovebox. For phase analysis and crystal structure determination, X-Ray diffractometer was used at room temperature (BRUKER D8 ADVANCE X-RAY DIFFRACTOMETER, Karlsruhe, Germany), Koç University (KUYTAM). CuK α radiation generated by 40kV of voltage and 40 mA of current were employed. Measurement parameters were chosen from (2 θ) 15° to 70° with a step size of 0.02° and a step time of 0.2 seconds. The diffraction pattern of KFeO₂ revealed that monophasic crystal structure of the synthesized product. All peaks are very well matched with the pure orthorhombic structure with the Pbc_a space group described in the structural database (File no: 04-013-8446, a= 5.59 b= 11.22 and c=15.93 Å). There was no sign of decomposition with the moisture. Decomposition of the KFeO₂ can be observed with the color change. Since the color of the KFeO₂ was olive green when it decomposes with the moisture in the air, iron oxide is formed and the color changes to the red.

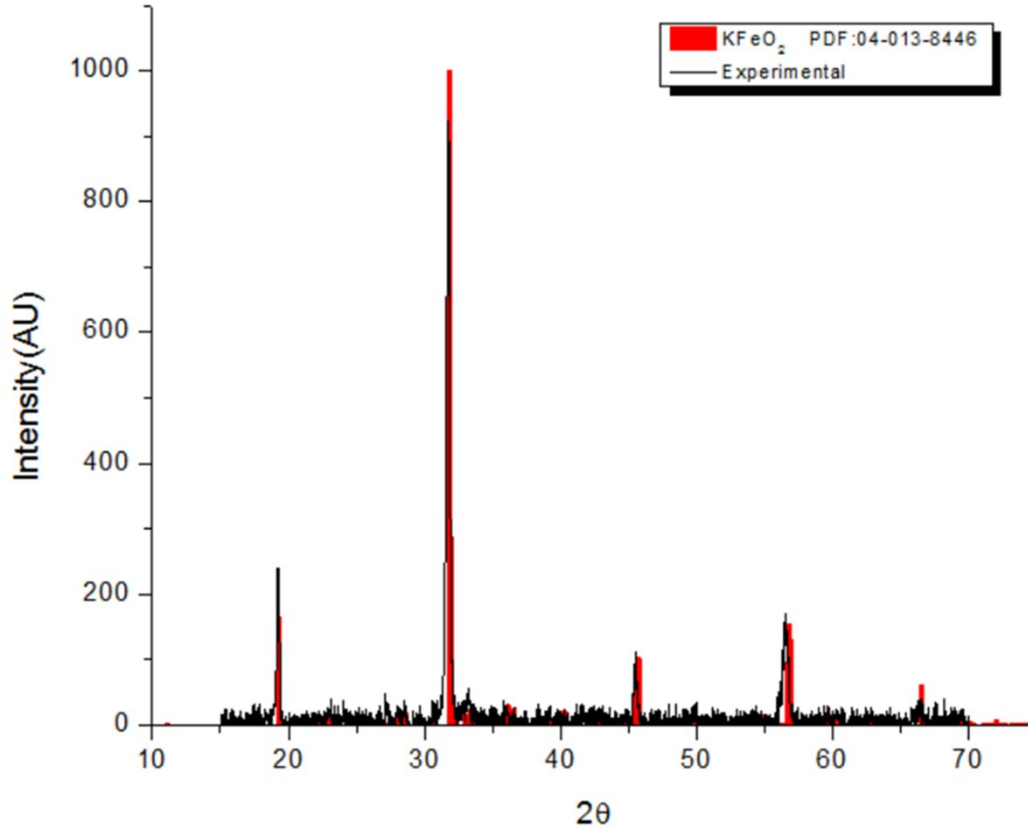


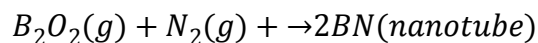
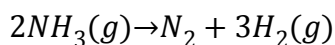
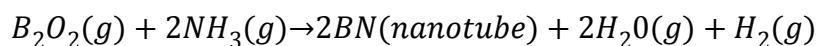
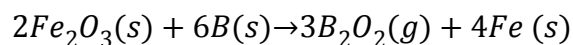
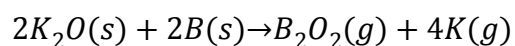
Figure S1: Phase analysis of KFeO₂

BNNT production

BNNTs production was carried out by growth vapor trap TCVD method. Schematic of the setup can be seen in Figure S2. In this configuration, close end inner quartz tube (2 cm in diameter and 50 cm in length) was placed inside the horizontal furnace against the gas flow to avoid trap growth vapor carried away from the substrate. Therefore reactive growth vapor which was formed reaction between precursors reached enough vapor pressure for nucleation on the substrate. The inner tube was prepared inside the glovebox to avoid KFeO₂ decomposition with moisture. Amorphous boron powder and KFeO₂ (2:1 mole ratio) were mixed in a mortar and

place inside the ceramic reaction boat (only half of it filled with powder). The top of the reaction boat was fully covered with the ceramic substrate, which was prepared by cutting the bottom of another empty reaction boat. Then, covered reaction boat was placed near to the closed end side of the inner quartz tube and sealed with silicone rubber stopper. After that, tube system was removed from the glovebox and placed inside the vertical furnace. Before the experiment was run, argon was introduced to the system to remove oxygen, and inner tube was opened under argon. Then, the system was heated under 200 ml/min NH₃ flow to 800 °C in one hour and kept for 2 hours.

Reaction temperature to form BNNT has determined around and over potassium boiling point related to the desorption of potassium from KFeO₂ phase with temperature and reducing atmosphere. Predicted reactions to synthesized BN are listed below.



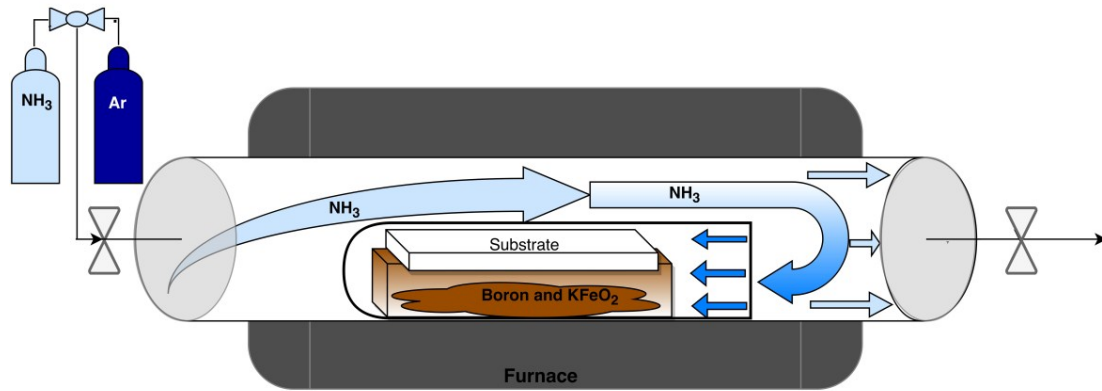


Figure S2: Vapor trap TCVD system setup

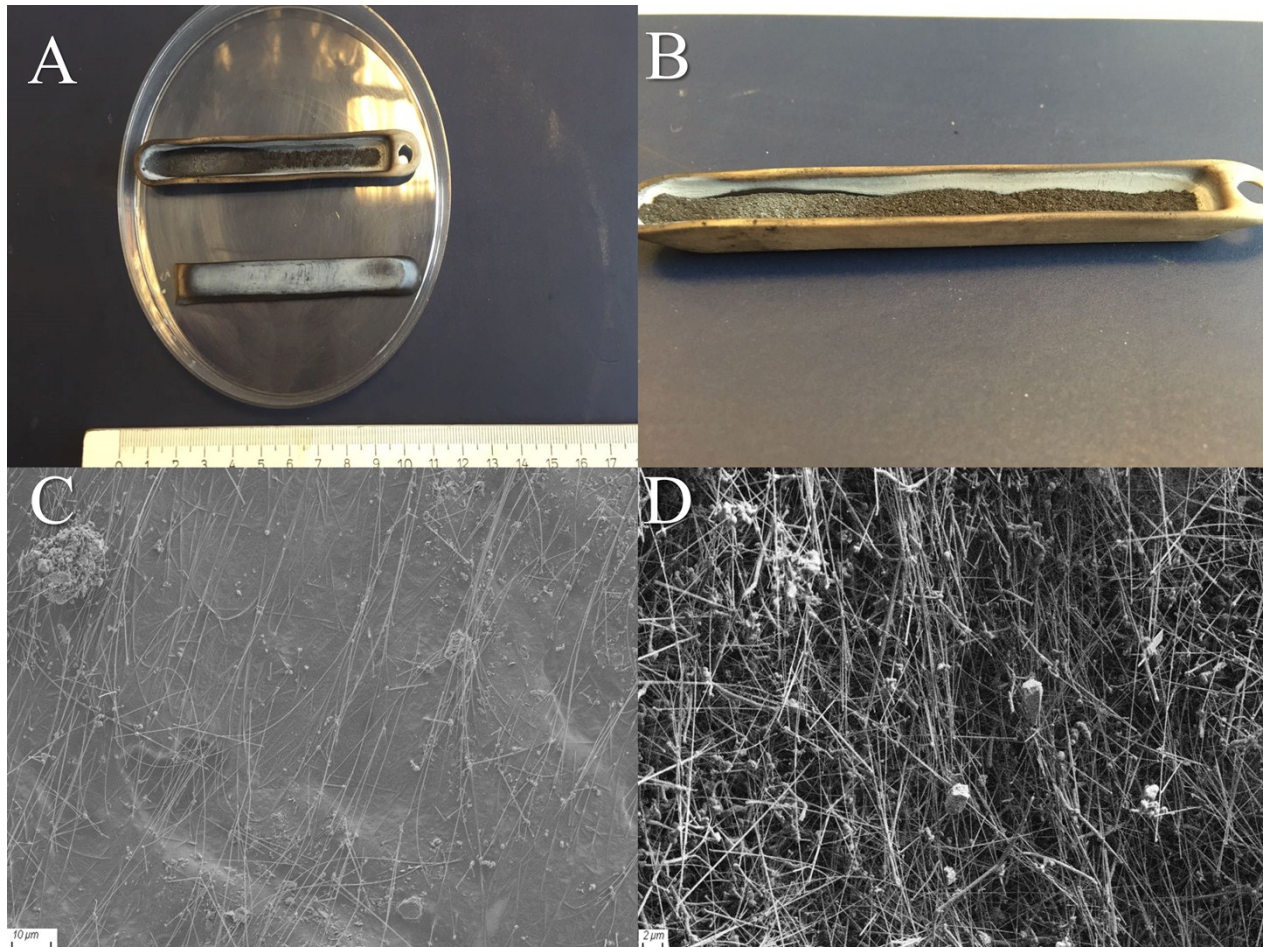


Figure S3: As synthesized BNNTs on the substrates A) Ceramic substrate (bottom of the empty crucible which was cut before and placed on the top of the combustion boat) B) walls of combustion boat C-D) SEM images of torn off substrate particles along with the nanotubes

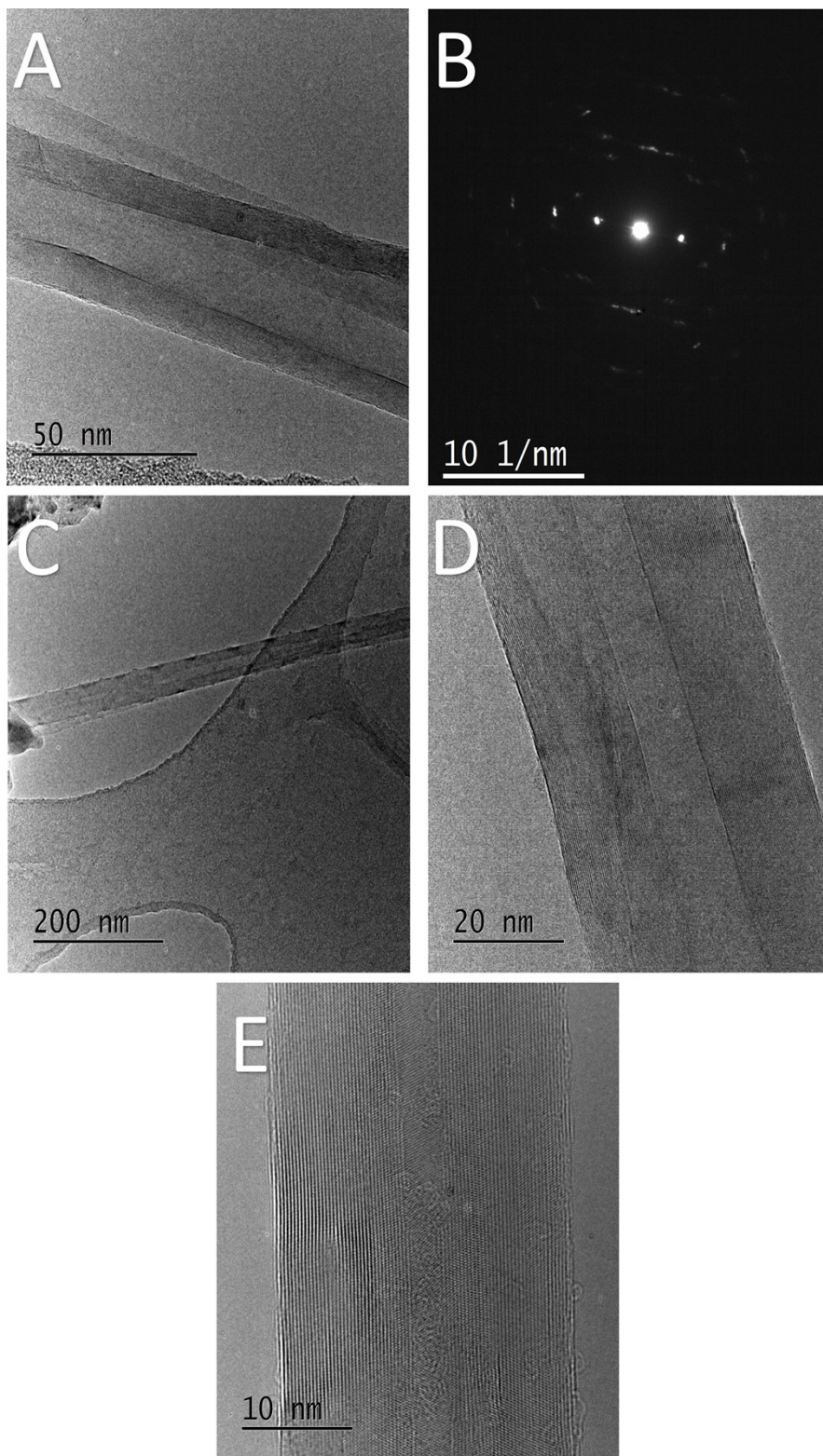


Figure S4: A) Higher magnification TEM image representing the contrast difference between tube walls and the center. B) SAED pattern of a typical BNNT. C-E) Additional TEM images of BNNTs

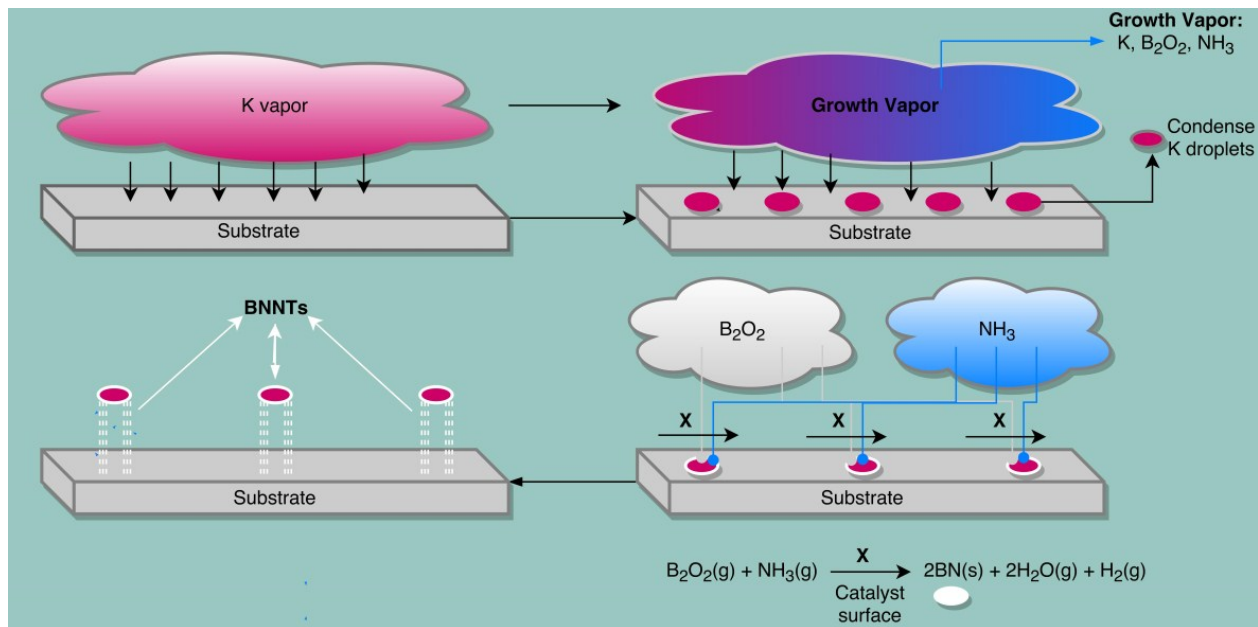


Figure S5: Schematics of possible VLS mechanism in this study

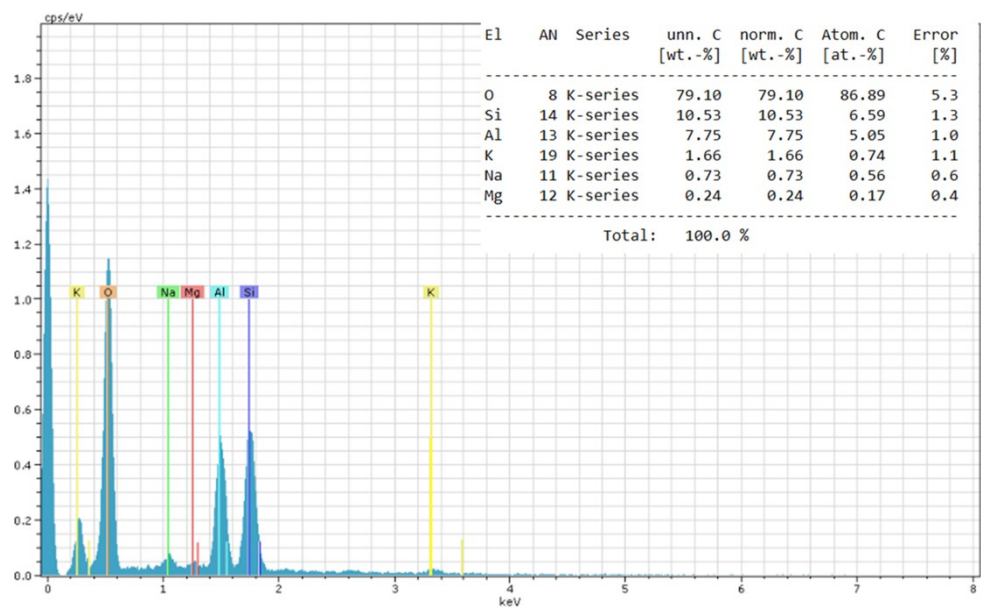


Figure S6: EDS spectra of ceramic crucible

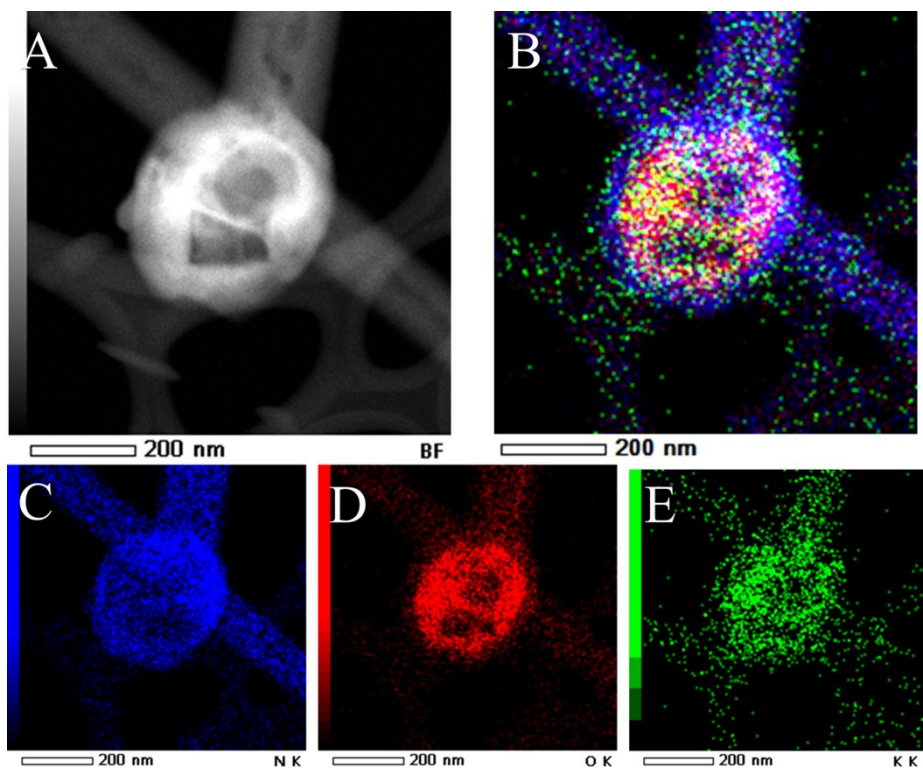


Figure S7: HAADF micrograph of nanotube tip, EDS map of C) potassium D) oxygen E) nitrogen F) overlay image of three elements (Core-shell structure) a day after the first measurement.

References

1. Tang, C.; Bando, Y.; Sato, T.; Kurashima, K. *Chemical Communications* **2002**, (12), 1290-1291.
2. Zhi, C.; Bando, Y.; Tan, C.; Golberg, D. *Solid State Communications* **2005**, 135, (1), 67-70.
3. Chee Huei, L.; Jiesheng, W.; Vijaya, K. K.; Jian, Y. H.; Yoke Khin, Y. *Nanotechnology* **2008**, 19, (45), 455605.
4. Lee, C. H.; Xie, M.; Kayastha, V.; Wang, J.; Yap, Y. K. *Chemistry of Materials* **2010**, 22, (5), 1782-1787.
5. Tang, C. C.; Bando, Y.; Sato, T. *Applied Physics A* **2002**, 75, (6), 681-685.
6. Tang, C.; Bando, Y.; Golberg, D. *Journal of Solid State Chemistry* **2004**, 177, (8), 2670-2674.
7. Golberg, D.; Bai, X. D.; Mitome, M.; Tang, C. C.; Zhi, C. Y.; Bando, Y. *Acta Materialia* **2007**, 55, (4), 1293-1298.
8. Wei, X.; Wang, M.-S.; Bando, Y.; Golberg, D. *Advanced Materials* **2010**, 22, (43), 4895-4899.
9. Yamaguchi, M.; Tang, D.-M.; Zhi, C.; Bando, Y.; Shtansky, D.; Golberg, D. *Acta Materialia* **2012**, 60, (17), 6213-6222.
10. Yang, H.; Yoshio, B.; Chengchun, T.; Chunyi, Z.; Takeshi, T.; Benjamin, D.; Takashi, S.; Dmitri, G. *Nanotechnology* **2009**, 20, (8), 085705.
11. Yang, H.; Jing, L.; Chengchun, T.; Yoshio, B.; Chunyi, Z.; Tianyou, Z.; Benjamin, D.; Takashi, S.; Dmitri, G. *Nanotechnology* **2011**, 22, (14), 145602.
12. Sinitskii, A.; Erickson, K. J.; Lu, W.; Gibb, A. L.; Zhi, C.; Bando, Y.; Golberg, D.; Zettl, A.; Tour, J. M. *ACS Nano* **2014**, 8, (10), 9867-9873.
13. Ferreira, T. H.; Silva, P. R. O.; Santos, R. G.; Sousa, E. M. B. *Journal of Biomaterials and Nanobiotechnology* **2011**, Vol.02No.04, 9.
14. Amir, P.; Chunyi, Z.; Yoshio, B.; Tomonobu, N.; Dmitri, G. *Nanotechnology* **2012**, 23, (21), 215601.
15. Seo, D.; Kim, J.; Park, S.-H.; Jeong, Y.-U.; Seo, Y.-S.; Lee, S.-H.; Kim, J. *Journal of Industrial and Engineering Chemistry* **2013**, 19, (4), 1117-1122.
16. Özmen, D.; Sezgi, N. A.; Balcı, S. *Chemical Engineering Journal* **2013**, 219, 28-36.
17. Li, L.; Liu, X.; Li, L.; Chen, Y. *Microelectronic Engineering* **2013**, 110, 256-259.
18. Kalay, S.; Yilmaz, Z.; Çulha, M. *Beilstein Journal of Nanotechnology* **2013**, 4, 843-851.
19. Maria Nithya, J. S.; Pandurangan, A. *RSC Advances* **2014**, 4, (51), 26697-26705.
20. Ahmad, P.; Khandaker, M. U.; Amin, Y. M. *Physica E: Low-dimensional Systems and Nanostructures* **2015**, 67, 33-37.
21. Wang, L.; Li, T.; Long, X.; Wang, X.; Xu, Y.; Yao, Y. *Nanoscale* **2017**, 9, (5), 1816-1819.